

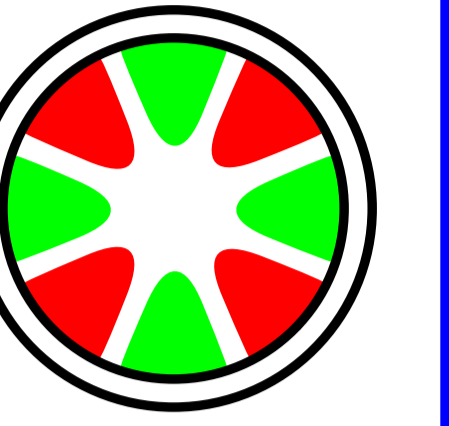
# Realization of the First Aplanatic Transmission Electron Microscope

I. Maßmann\*, S. Uhlemann\*, H. Müller\*, P. Hartel\*, J. Zach\*, M. Haider\*, Y. Taniguchi\*\*, D. Hoyle\*\*\* and R. Herring\*\*\*\*.

\*Corrected Electron Optical Systems GmbH, Englerstr. 28, D-69126 Heidelberg, Germany.  
 \*\*Hitachi High-Technology Corporation, 882, Ichige, Hitachinaka, Ibaraki, 312-8504 Japan.  
 \*\*\*Hitachi High-Technology Ltd., 89 Galaxy Blvd. Suite 14, Toronto, Ontario, Canada, M9W 6A4.  
 \*\*\*\*University of Victoria, P.O. Box 3055, Victoria, B.C., V8W 3P6 Canada.

CEOS

Corrected Electron Optical  
Systems GmbH



## Background

### Introduction

Today it is not unusual that electron microscopes are equipped with CCD cameras resolving 4kx4k pixels or more. The high-resolution field of view of such a microscope is no longer limited by the CCD's modulation transfer function but by off-axial aberrations. The dominating aberration is the off-axial coma  $B_3 = B_{2\bar{\gamma}}$  which can be corrected with a new aplanatic hexapole-type CEOS  $C_5/B_3$ -corrector system called B-COR. Additionally the novel design is free of intrinsic unround axial aberrations up to the fifth order.

### Off-axial aberrations

Off-axial aberrations can be defined as a function of the lateral position  $\gamma = x + iy$  and  $\bar{\gamma} = x - iy$ :

$$K(\gamma, \bar{\gamma}) = \gamma K_\gamma + \bar{\gamma} K_{\bar{\gamma}}$$

Isotropic/anisotropic magnification	$A_{0\gamma}$	$A_{0\bar{\gamma}}$
Image inclination	$C_{1\gamma}$	
Off-axial two-fold astigmatism	$A_{1\gamma}$	$A_{1\bar{\gamma}}$
Off-axial coma	$B_{2\gamma}$	$B_{2\bar{\gamma}} = B_3$
Off-axial three-fold astigmatism	$A_{2\gamma}$	$A_{2\bar{\gamma}}$

### High-resolution field of view

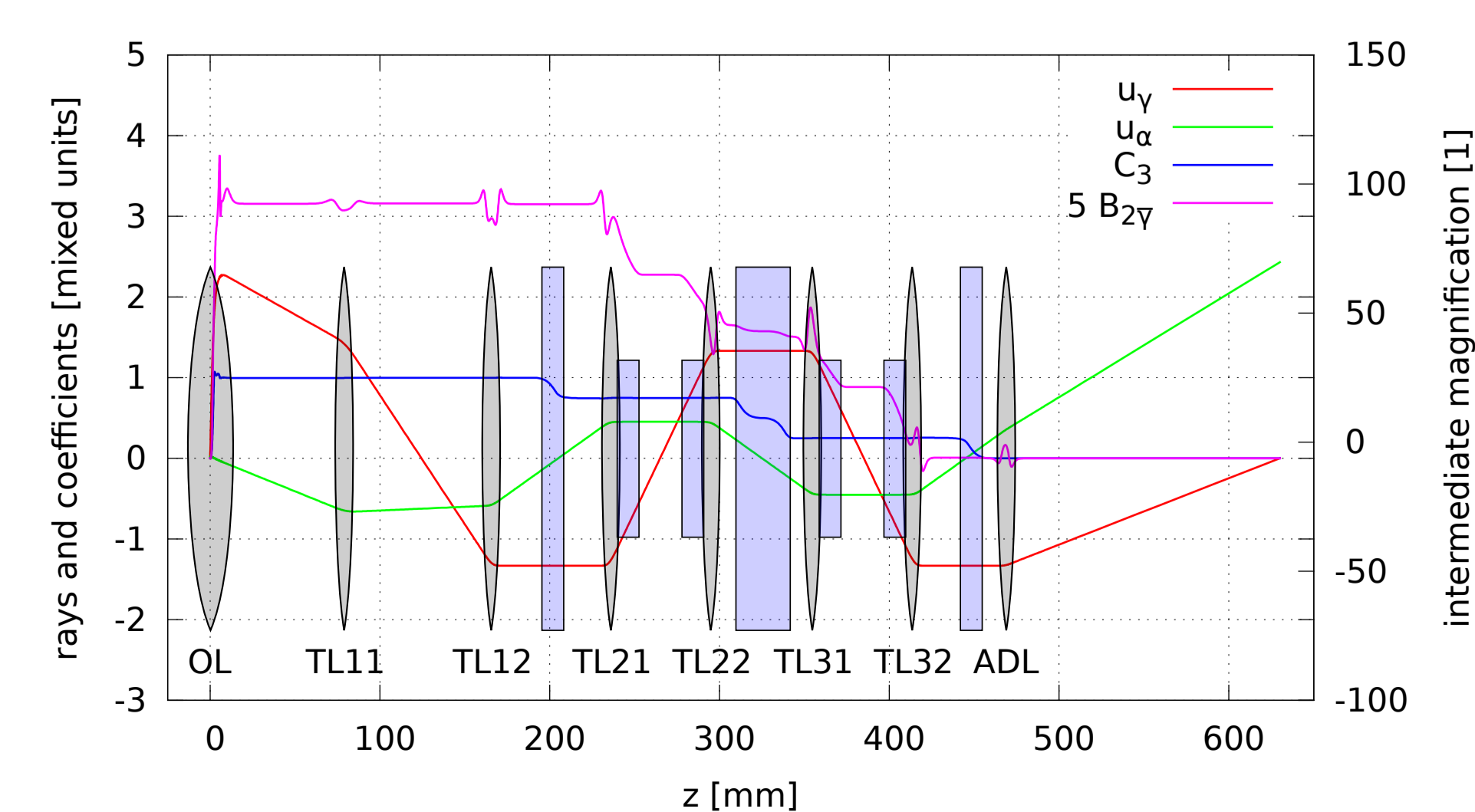
For single-gap magnetic round lenses the azimuthal component of  $B_{2\bar{\gamma}}$  cannot be zero. A typical value of 0.7 limits the aberration-free field of view  $D_0$  according to this rule of thumb [3]:

$$D_0 < \frac{1}{|B_{2\bar{\gamma}}| \lambda^2 g_{max}^3}$$

Example: Assume a system that can transfer spatial frequencies up to  $g_{max} = 15 \text{ nm}^{-1}$  with a residual phase shift less than  $\frac{\pi}{4}$ , 300 kV acceleration voltage ( $\lambda = 1.969 \text{ pm}$ ) and only the unavoidable  $|B_{2\bar{\gamma}}| > 0.7$  present. For such a system the aberration-free field of view can not be larger than  $D_0 = 110 \text{ nm}$  even if all other axial and off-axial aberrations are zero. Practically the situation is much worse since a large number of small residual aberrations has to be considered.

### The B-COR

The hexapole-type  $C_5/B_3$ -corrector is based on a three hexapole design. It corrects for the spherical aberration and the off-axial coma of the imaging system. By design the novel hexapole corrector is free of intrinsic six-fold astigmatism  $A_5$ . The small negative fifth-order spherical aberration  $C_5$  is beneficial for positive phase contrast over a broad range of spatial frequencies. The  $C_5/B_3$ -corrector provides means to correct for all parasitic axial aberrations up to fourth order and off-axial aberrations up to third order. Hence, this corrector for the first time enables the realization of a fully aplanatic and fifth-order corrected CTEM.



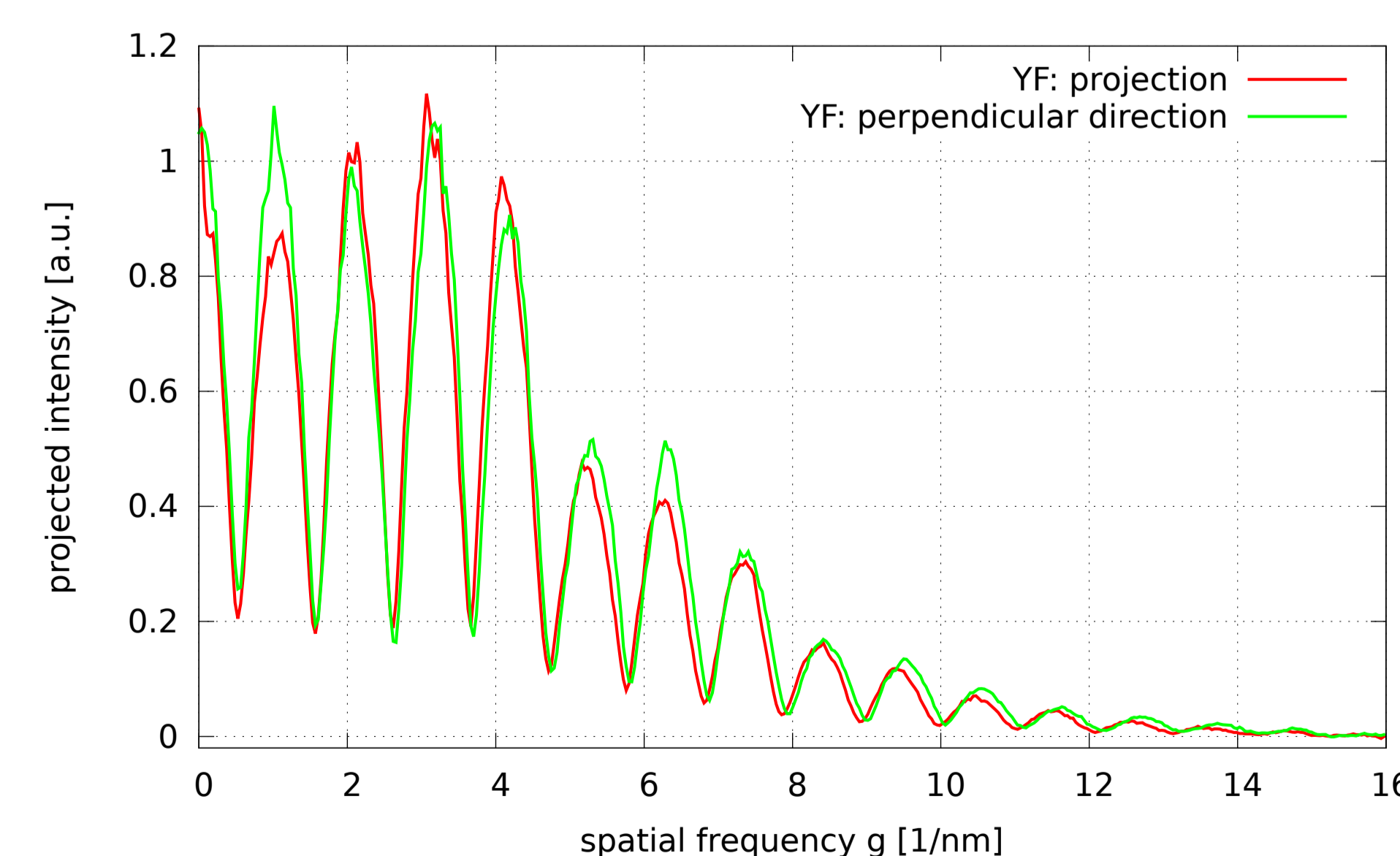
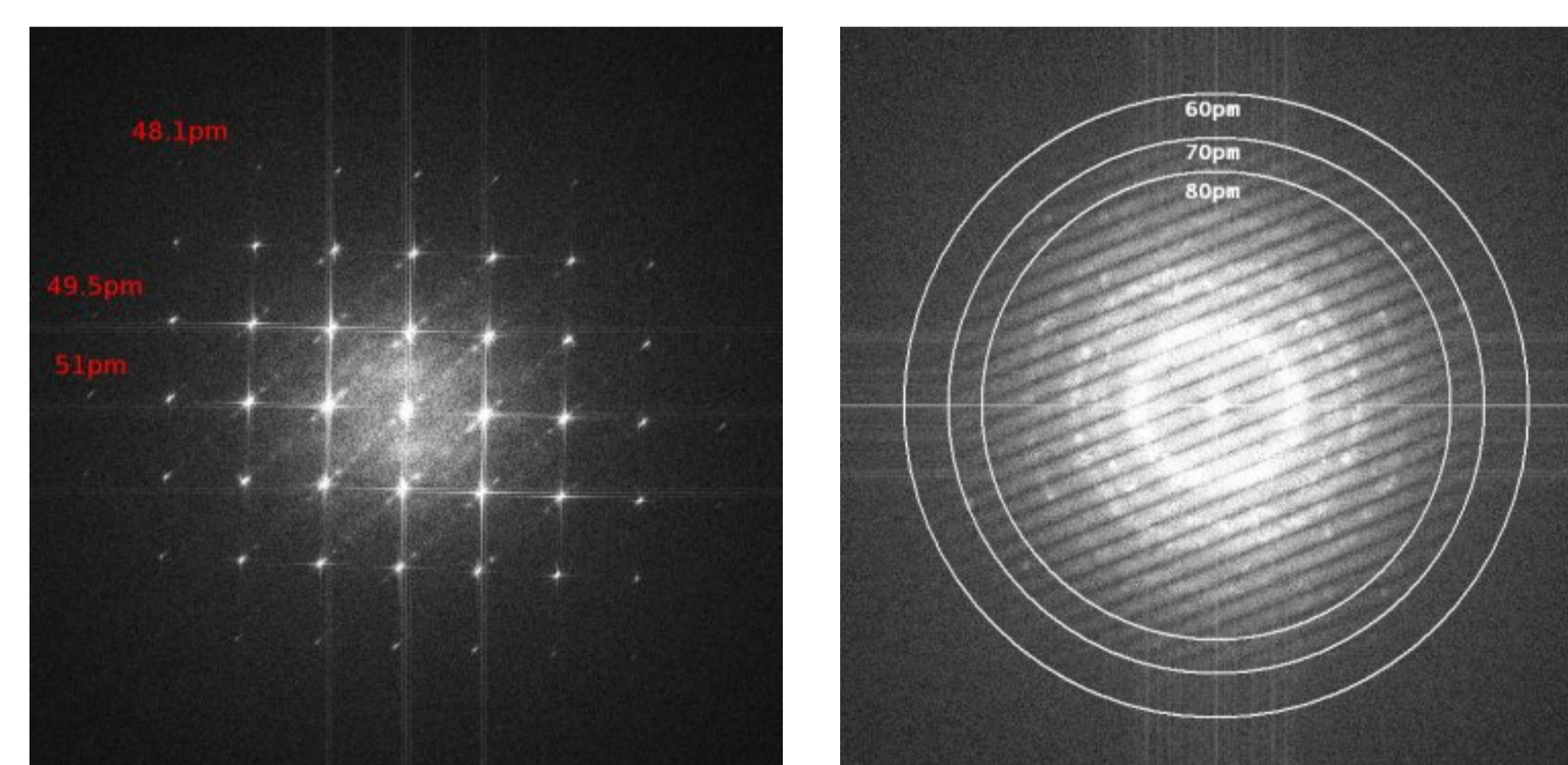
## Experimental Results

### Hitachi HF3300V with CEOS B-COR

The next-generation hexapole corrector for the conventional TEM has been integrated into the new Hitachi HF3300V TEM equipped with a cold field emission gun [4]. Due to its high-brightness with small intrinsic focus spread and very high mechanical and electrical stability the system provides a very competitive information limit. The quality of the Thon rings in the diffractograms is exceptionally good and delivers very accurate and reliable information about the residual aberrations of the system.



### Oriented gold and Young's fringes @ 300kV

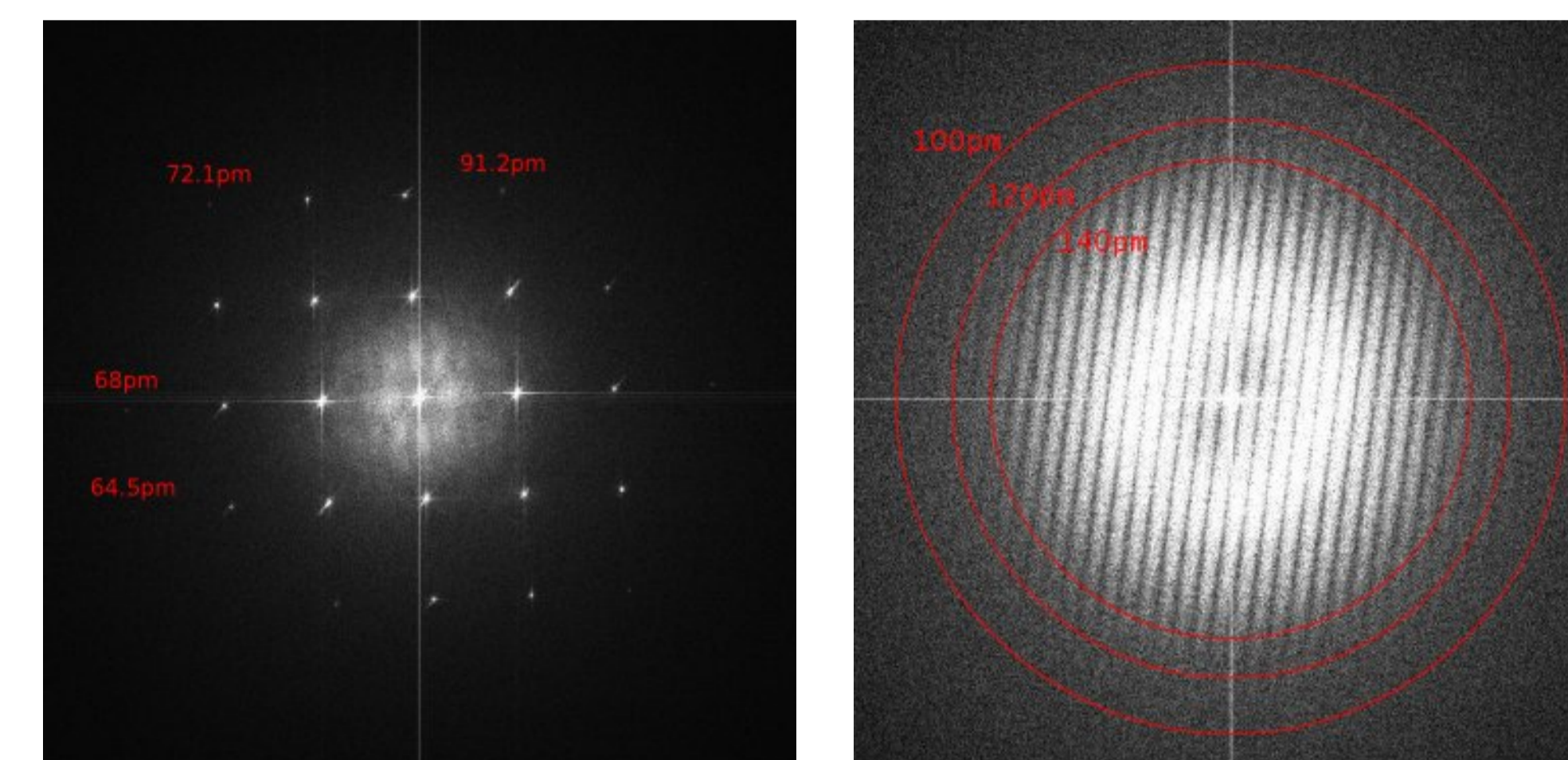


The plot shows a projection of the Young's fringe pattern above. It has been recorded with a thin tungsten specimen at 300kV and shows information transfer up to  $15 \text{ nm}^{-1}$  in both directions.

### Conclusion

The performance of the Hitachi HF3300V with the CEOS B-COR and the automated measurement and correction of the axial and off-axial aberrations opens the door for new exciting experiments with a large aberration free field of view.

### Oriented gold and Young's fringes @ 60kV



### Focus spread

The focus spread has been measured by taking Young's fringe images with an illumination tilt of  $3^\circ$ . By comparing the damping envelope between the tilted and the untilted image the total root mean square defocus spread can be measured to be  $\text{rms}(C_1) = 1.35 \text{ nm} \pm 0.1 \text{ nm}$ . The chromatic focus spread is given by the measured energy width of  $dE(\text{fwhm}) = 0.45 \text{ eV}$  [4] and the chromatic aberration  $C_C = 2.28 \text{ mm}$  is calculated to be  $\text{rms}(C_1) = 1.46 \text{ nm}$ .

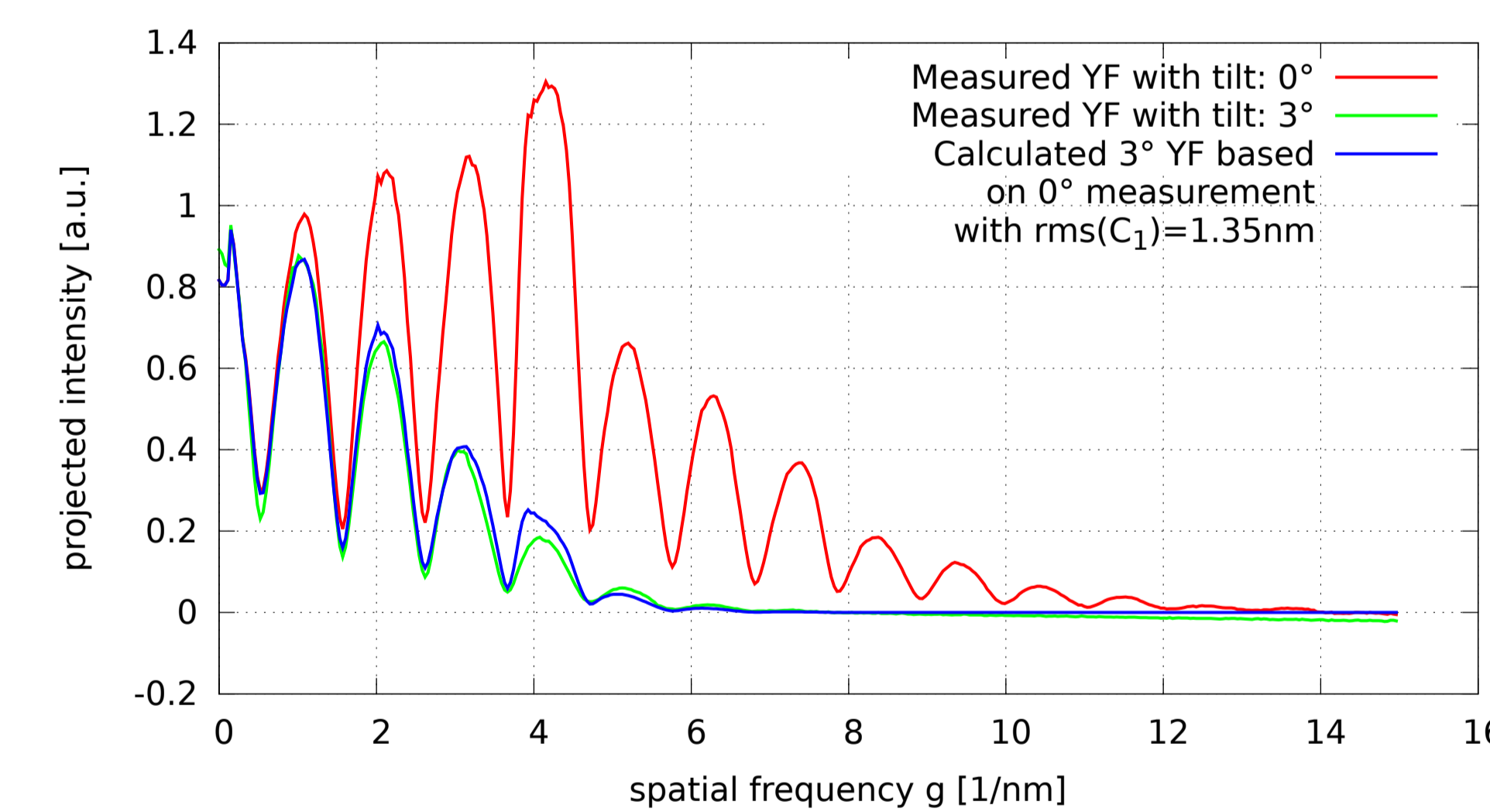
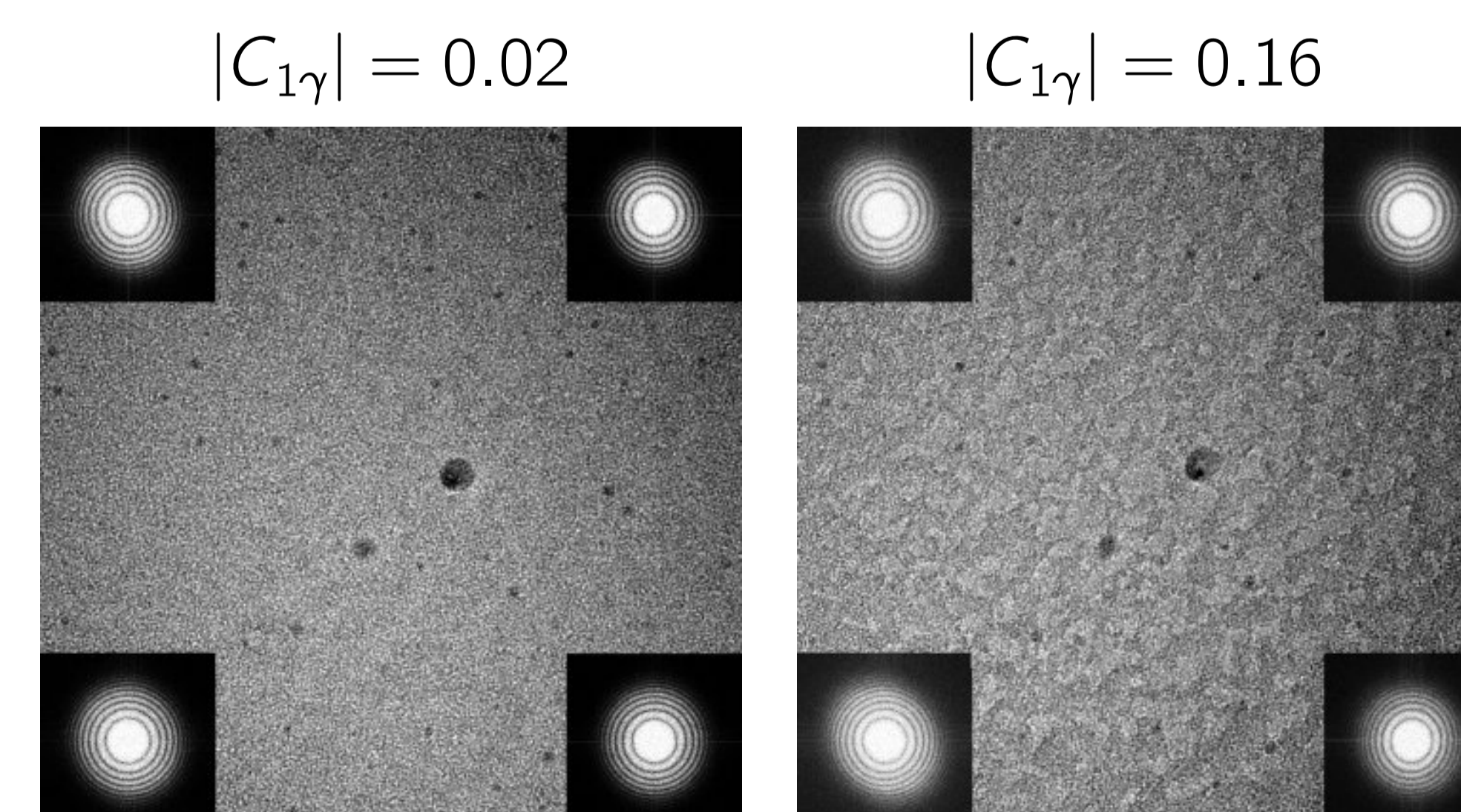


### Image inclination $C_{1\gamma}$

With the B-COR the image inclination can be adjusted. This allows to compensate for a linear focus wedge over the image. Between the two pictures below only the alignment of the corrector has been changed not the mechanical position or tilt of the specimen. The left picture is taken with  $|C_{1\gamma}| = 0.02$  or a tilt of  $2^\circ$ . The right picture is taken with  $|C_{1\gamma}| = 0.16$  which corresponds to a specimen tilt of  $18^\circ$ .



### References

- [1] M. Haider, et al. Advances in Imaging and Electron Physics 153, 43-119, 2008.
- [2] M. Haider, et al. Microsc. Microanal. 16, 393-408, 2010.
- [3] H. Müller, et al., Nucl. Instr. Meth. A 645 (2011) 20-27
- [4] T. Sato, et al. Hitachi Rev. 57(3), 132-135, 2008.
- [5] S. Uhlemann, et al. Ultramicroscopy 72, 109-119, 1998.

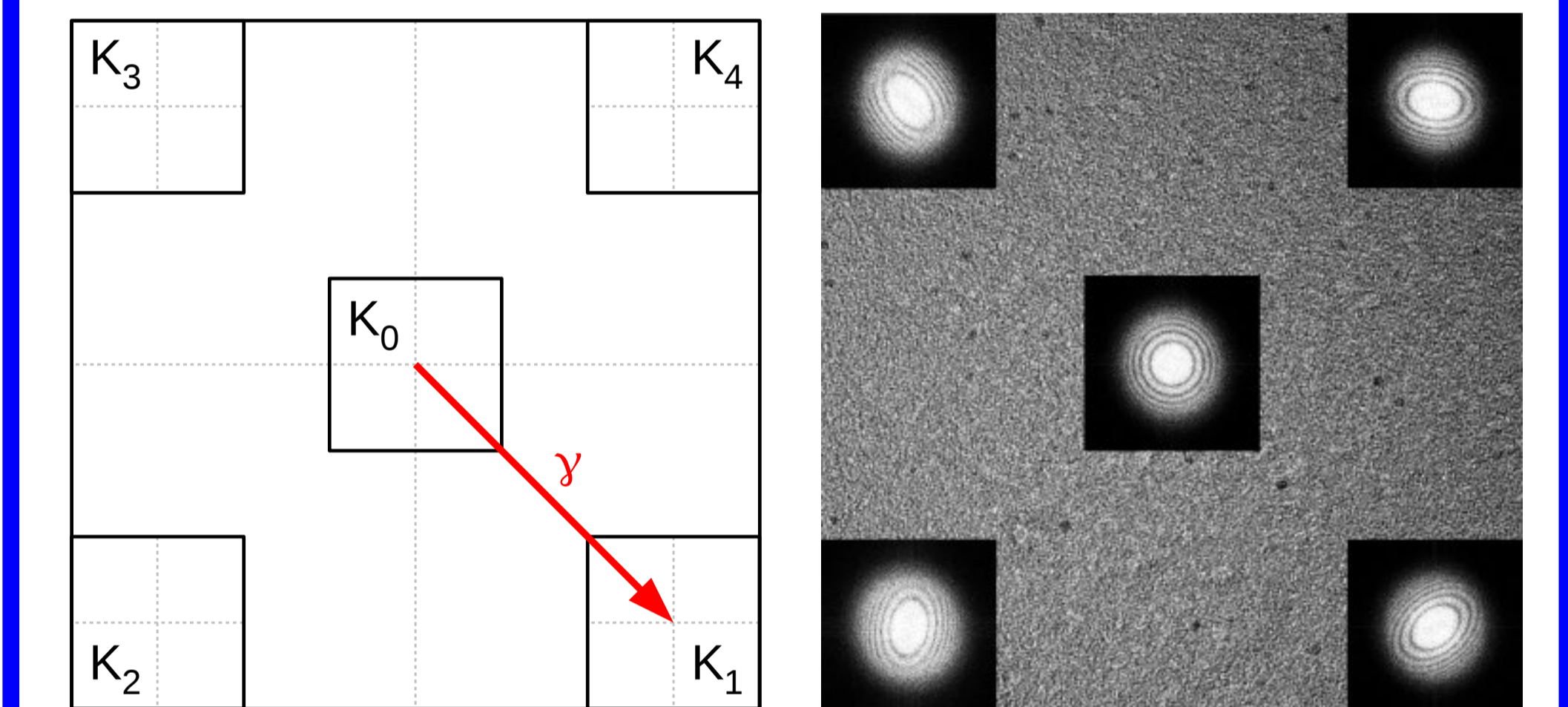
## Alignment

### Measuring off-axial aberrations

Aberrations are measured by splitting the  $2k \times 2k$  pixel image into five sub-regions with  $512 \times 512$  pixel each. The region in the center of the image is used to calculate the axial aberrations and the four regions in the corners are used for the off-axial aberrations. While evaluating a Zemlin tableau for each region the axial aberration coefficients  $K_1$ ,  $K_2$ ,  $K_3$  and  $K_4$  are calculated independently. From these coefficients the off-axial coefficients  $K_\gamma$  and  $K_{\bar{\gamma}}$  can be calculated by using  $K_{m\bar{n}} = K_m - K_n$  with  $m, n = 1, 2, 3, 4$ :

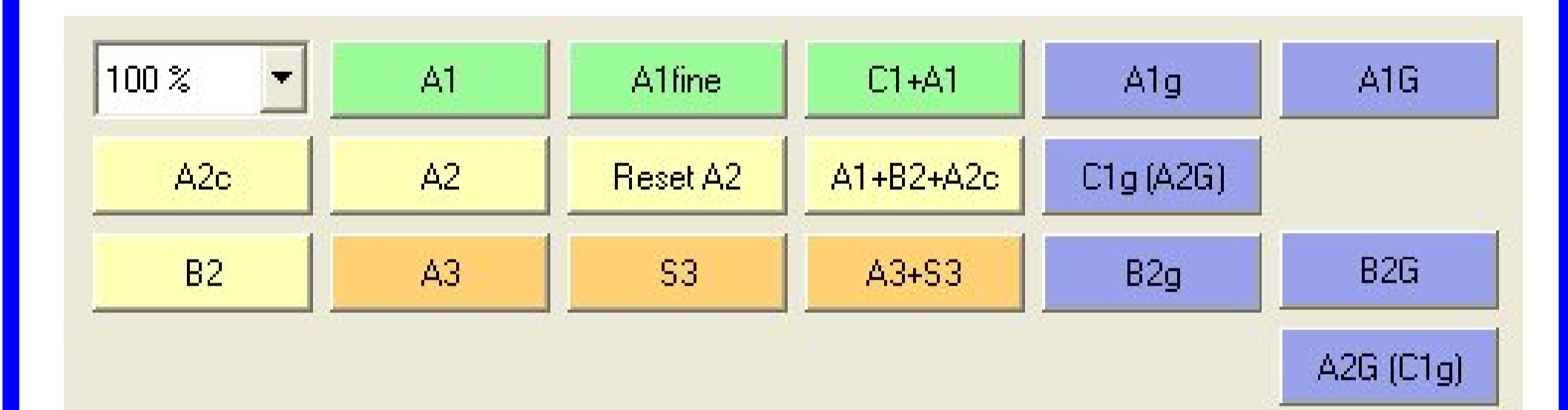
$$K_\gamma = \frac{1}{4\sqrt{2}|\gamma|} [(K_{13} - K_{24}) - i(K_{13} + K_{24})]$$

$$K_{\bar{\gamma}} = \frac{1}{4\sqrt{2}|\bar{\gamma}|} [(K_{13} - K_{24}) + i(K_{13} + K_{24})]$$



### Aligning the corrector

The measured aberrations can be corrected by using the auto alignment buttons provided by the corrector software:



### Residual aberrations

The off-axial coma  $B_{2\bar{\gamma}}$  has been reduced by almost a factor of 20 compared to the uncorrected objective lens. The six-fold astigmatism  $A_5$  is zero within its error bars.

coeff.	value	abs. err.	coeff.	value	abs. err.
$C_{1\gamma}$	0.117	-120°	0.005		
$A_{1\gamma}$	0.007	-137°	0.009	$A_{1\bar{\gamma}}$	0.011 / -174°
$B_{2\gamma}$	0.03	130°	0.09	$B_{2\bar{\gamma}}$	<b>0.037</b> / 164°
$A_{2\gamma}$	0.23	-78°	0.16	$A_{2\bar{\gamma}}$	0.13 / -96°

coeff.	value	abs. err.
$C_1$	-180 nm	1 nm
$A_1$	4 nm / 159°	1 nm
$B_2$	23 nm / 119°	17 nm
$A_2$	13 nm / 140°	19 nm
$C_3$	<b>-1.3 μm</b>	1.3 μm
$A_3$	448 nm / -127°	170 nm
$S_3$	344 nm / 64°	100 nm
$A_4$	5.3 μm / 94°	3.4 μm
$B_4$	6.4 μm / -134°	4 μm
$D_4$	3 μm / -63°	2.1 μm
$C_5$	-1.4 mm	0.5 mm
$A_5$	<b>37 μm</b> / 45°	71 μm